

WRF Model Simulations of Aqueous Chemistry in the July 10 STERAO Deep Convective Storm

Si-Wan Kim, Mary C. Barth, William C. Skamarock

National Center for Atmospheric Research
Boulder, Colorado, USA

1. INTRODUCTION

Model studies have shown that convective injections of peroxides (H_2O_2 , CH_3OOH) and formaldehyde (CH_2O) in the boundary layer (BL) to the upper troposphere (UT) can produce HOx and ozone in the UT (Chatfield and Crutzen, 1984; Prather and Jacob, 1997). Peroxides and formaldehyde is reservoir species in the ozone chemical reaction system. Ozone precursors include hydroperoxy radicals that are stored in peroxides and CH_2O . Cohan et al. (1999) addressed the importance of deep convection on the BL air venting and scavenging of H_2O_2 and CH_3OOH using aircraft observation in the marine environment. They found that mixing ratios of CH_3OOH in convective outflow at 8-12 km altitude are enhanced on average by a factor of 6 relative to background, while mixing ratios of H_2O_2 are enhanced by less than a factor of 2. The estimated scavenging efficiency of H_2O_2 is 55-70%, while that of CH_3OOH is negligible. These aircraft observations were not exactly coincident with convective events in time, which puts some limitations on the interpretation of data due to uncertainties in chemical reactions, advection and convection processes. To understand interactions among convection, microphysics, and aqueous chemistry, a modeling framework that is complementary to observations needs to be developed.

Here we introduce the Weather and Research Forecast (WRF) model coupled with aqueous chemistry and microphysical transfer processes. We examine the importance of cloud physics and chemistry on peroxides and CH_2O concentrations by simulating the 10 July 1996 STERAO storm which was observed in northeastern Colorado.

2. MODEL DESCRIPTION

The WRF model is the host meteorological model. The model solves the conservative (flux-form), nonhydrostatic compressible equations (Skamarock et al., 2001) using a split-explicit

time-integration method based on a 3rd order Runge-Kutta scheme (Wicker and Skamarock, 2002). Scalar transport is integrated with the Runge-Kutta scheme using 5th order (horizontal) and 3rd order (vertical) upwind-biased advection operators. Transported scalars include water vapor, cloud water, rain, cloud ice, snow, graupel (or hail), and chemical species. The WRF model exactly conserves mass and scalar mass to machine round off. Further information concerning the equations and integration scheme can be found at http://www.mmm.ucar.edu/individual/skamarock/wrf_equations_eulerian.pdf and the meteorological model and further documentation can be found at <http://wrf-model.org>. The ice microphysics parameterization is that described by Lin et al. (1983). For the simulations performed here, hail hydrometeor characteristics ($\rho_h = 0.9 \text{ g cm}^{-3}$, $N_o = 4 \times 10^4 \text{ m}^{-4}$) are used.

The model is configured to a 120 x 120 x 20 km domain with 121 grid points in each horizontal direction (1 km resolution) and 51 grid points in the vertical direction with a variable resolution beginning at 50 m at the surface and stretching to 1200 m at the top of the domain. A description of the meteorological scenario and transport of passive tracers is found in Skamarock et al. (2000) for the 10 July 1996 STERAO storm. We initialize the model environment and the initiation of convection in the same manner as Skamarock et al.

The gas chemistry represents daytime chemistry of 15 chemical species, methane, carbon monoxide (CO), ozone (O_3), hydroxyl radical (OH), hydroperoxy radical (HO_2), nitrogen dioxide, nitric oxide, nitric acid (HNO_3), H_2O_2 , CH_3OOH , CH_2O , formic acid (HCOOH), sulfur dioxide (SO_2), aerosol sulfate, and ammonia (NH_3). The aqueous chemistry is computed for the cloud water and rain assuming a pH of 4.5. Most chemical species are initialized with values measured in the inflow region of the storm; other species are estimated from values found in the literature or from the July monthly-mean mixing ratio for northeastern Colo-

rado calculated by the 3-dimensional global transport model, MOZART (Brasseur et al., 1998). The chemical mechanism is solved with an Euler backward iterative approximation using a Gauss-Seidel method with variable iterations. A convergence criterion of 0.01% is used for all the species.

3. RESULTS

The simulated storm has radar reflectivity comparable to the observed storm (Figure 1, maximum reflectivity greater than 50 dBZ). Observed radar reflectivity obtained from the CSU CHILL radar reveals a multi-cellular system (2 cells), as does the radar reflectivity calculated from the model results (3 cells). The observed storm reaches lower stratosphere, while the simulated storm does not develop to that height.

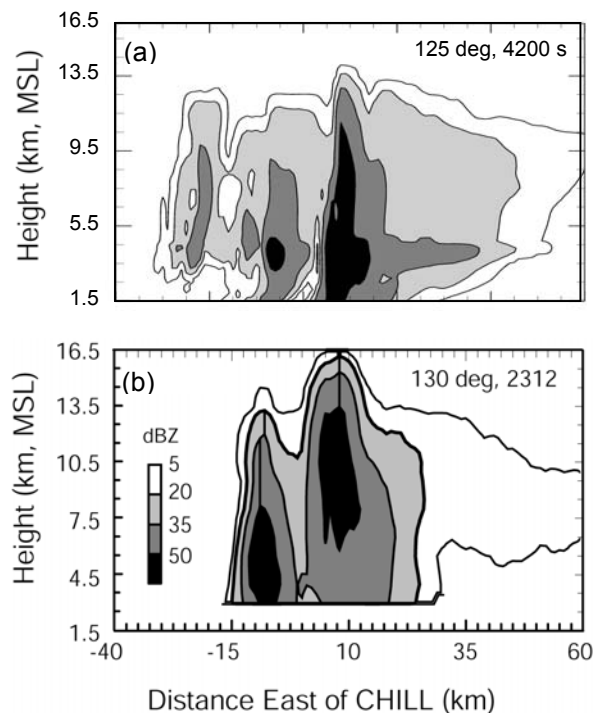


Figure 1. Radar reflectivity of a cross section through the storm from (a) simulation at t = 4200 s and (b) CHILL radar.

The modeled storm at t = 4200 s is oriented in a northwest-southeast direction (Figure 2). The cores are composed mostly of cloud water and hail with rain situated below the hail. The anvil is composed of snow and ice. Simulated CO and O₃ are compared with aircraft observation near the anvil region in Figure 3. These plots illustrate good agreement between our model results and observation. Due to convective pumping, CO (O₃)

concentrations are greater (smaller) in the anvil region compared to the background UT.

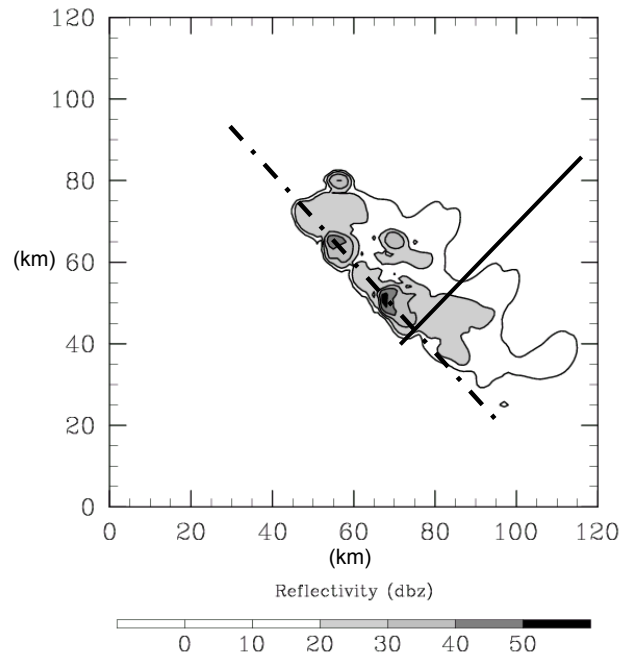


Figure 2. Horizontal radar reflectivity at 11.5 km altitude (simulation time 4200 s). Solid line represents aircraft flight path near this time, and dash-dotted line represents vertical cross section line for the calculation of scavenging coefficients.

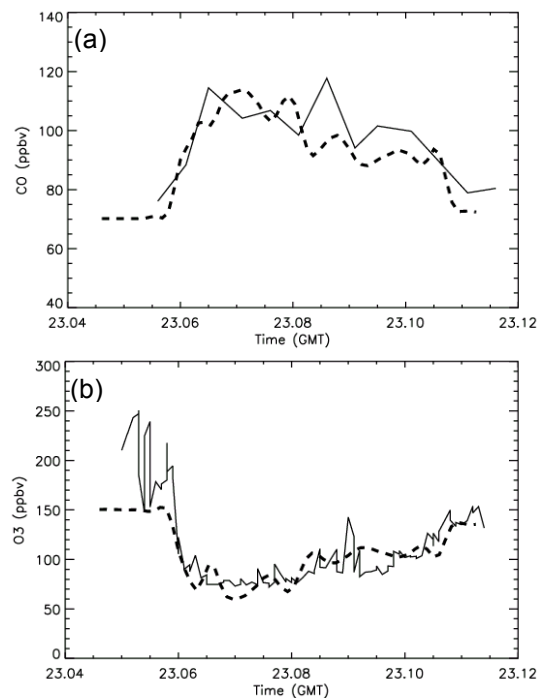


Figure 3. UND Citation (aircraft) (a) CO and (b) O₃ concentrations for anvil passes closest to the southeastern-most cell (solid line in Figure 2) from observations (solid lines) and model results (dashed lines).

To examine the importance of convective pumping of soluble and reactive chemical species, the total concentration (gas + cloud water + cloud ice + rain + snow + hail) of peroxides, CH_2O , HCOOH , HOx species, NO_x , and SO_2 across the anvil (such as is shown in Figure 3) are plotted in Figure 4.

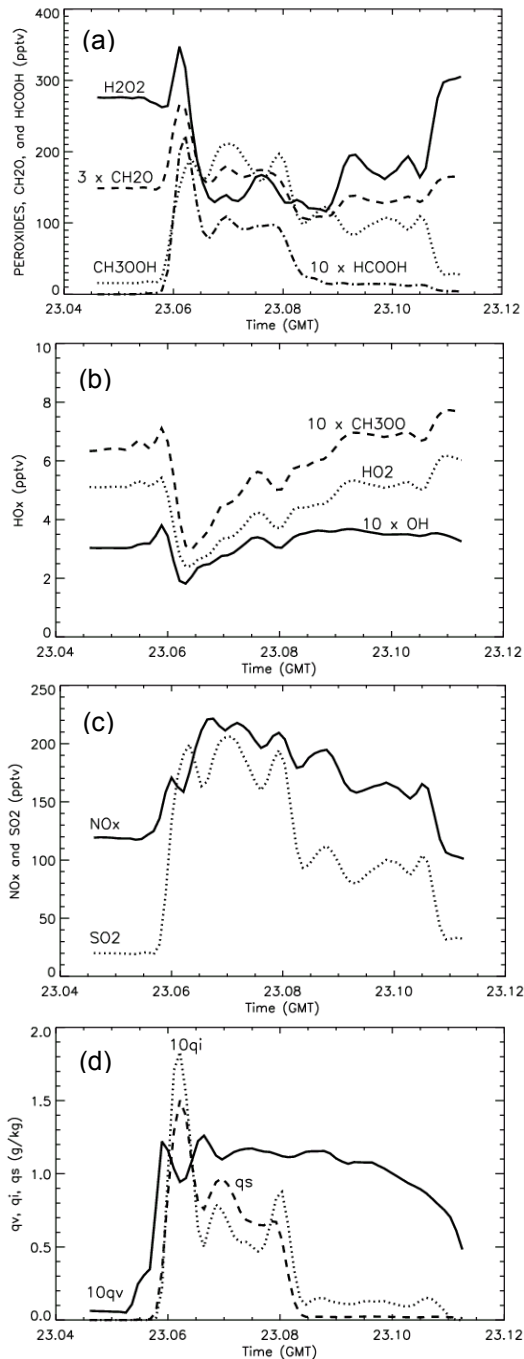


Figure 4. Concentration distribution of (a) peroxides, CH_2O , HCOOH , (b) HOx, (c) NO_x , SO_2 , and (d) water species across the anvil (following solid line in Figure 3).

At $z = 11.6$ MSL, the anvil is composed of snow and cloud ice (Figure 4d), indicating that the chemical species at this location resides in the gas, ice, and snow reservoirs. In the anvil CH_3OOH concentrations are more than ten times background concentration, while H_2O_2 and CH_2O concentrations are generally smaller than background concentrations. HOx species concentration within the anvil are less than background values. NO_x and SO_2 increase to twice and ten times background concentration across the anvil.

The CH_3OOH increase in the convective outflow agrees well with Cohan et al. (1999). However, increases in H_2O_2 and CH_2O are not found in these simulations contrary to Cohan et al.'s assumption. Aqueous chemistry has been shown to deplete peroxy radicals and CH_2O and to produce HCOOH (Barth et al., 2003). Thus, soluble species are dissolved into the cloud water at low and mid-levels of the convective cores. Aqueous reactions in this region modify the species' concentration while the transfer of the species among hydrometeors redistributes the species either to the ice in snow which are transported to the anvil or to the hail which falls and melts to form rain.

To understand how much solubility and aqueous chemistry affect the distribution of chemical species, we calculate each species' scavenging efficiency, which are determined by a two-component mixture method (Cohan et al., 1999). CO is used as a tracer and the boxes in Figure 5 are used for defining representative concentrations in BL, UT, and convective outflow regions. The spatial distribution of the total mixing ratio of CO indicates transport of the species from the BL to the UT. The scavenging efficiencies are summarized in Table 1, ordered by the magnitude of the solubility coefficient. The calculated scavenging efficiencies are about the same for species with solubility coefficients ranging from 6300 M/atm (CH_2O) to 10^{11} M/atm (HNO_3). It should be noted that significant uncertainties in the calculated scavenging efficiency occur when non-uniform concentrations occur in any of the analysis boxes. For example, gradients in the boundary layer concentration or the convective outflow concentration increase the uncertainty of the calculated scavenging efficiency.

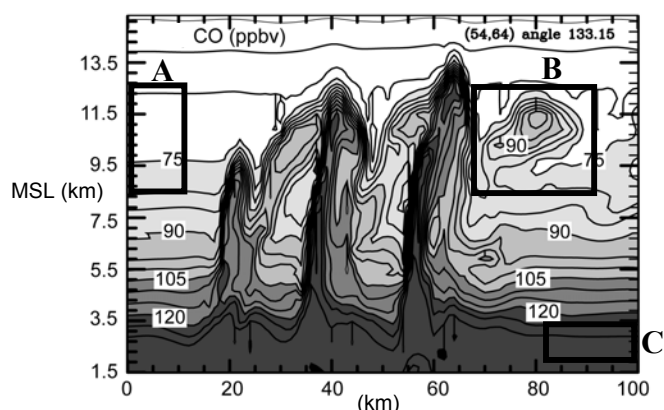


Figure 5. Cross-section of the CO mixing ratio at $t = 4200$ s. Total concentration (gas + cloud water + rain + ice + snow + hail) is shown. Boxes are defined for the calculation of scavenging efficiency. Box labeled A stands for UT background, box B for convective outflow, and box C for BL background.

Table 1. Concentrations averaged over box A, B, and (Figure 5), and scavenging efficiency of soluble species.

Species	BL (pptv)	UT (pptv)	CONV (pptv)	Scavenging efficiency
CO	130.1	71.7	91.6	Tracer
NO _x	274.7	79.9	140.1	0.067
CH ₃ OOH	428.3	35.9	149.6	0.139
SO ₂	843.9	43.8	150.7	0.577
CH ₂ O	1062.9	70.3	107.0	0.833
H ₂ O ₂	2304.9	413.4	410.6	0.824
NH ₃	382.5	2.2	20.8	0.851
HNO ₃	860.1	525.5	381.0	0.881

4. CONCLUSIONS

Aqueous and gas-phase chemistry as well as the transfer of dissolved chemical species among hydrometeors have been added to the WRF model. The results of the simulations show the importance of both cloud physics and cloud chemistry on the spatial distribution of soluble species. Other factors, such as cloud-modified photolysis frequencies, lightning-production of NO_x, and interactions between gas and ice phases, could also influence the spatial distribution of chemical species. These processes will be implemented in the future.

5. ACKNOWLEDGMENTS

The National Center for Atmospheric Research is operated by the University Corporation for Atmospheric Research under the sponsorship of the National Science Foundation.

6. REFERENCES

- Barth et al., 2003: Summary of the cloud chemistry modeling intercomparison: Photochemical box model simulation, *J. Geophys. Res.*, **108**, 4214-4304.
- Brasseur, G. P., et al., 1998: MOZART: A global chemical transport model for ozone and related chemical tracers, Part 1. Model Description, *J. Geophys. Res.*, **103**, 28,265-28,289.
- Chatfield, R. B., and P. J. Crutzen, 1984: Sulfur dioxide in remote ocean air: Cloud transport of reactive precursors, *J. Geophys. Res.*, **89**, 7111-7132.
- Cohan, D. S., et al., 1999: Convective injection and photochemical decay of peroxides in the tropical upper troposphere: methyl iodide as a tracer of marine convection, *J. Geophys. Res.*, **104**, 5717-5724.
- Lin, Y.-L., et al., 1983: Bulk parameterization of the snow field in a cloud model, *J. Clim. Appl. Meteor.*, **22**, 1065-1092.
- Prather, M. J., and D. J. Jacob, 1997: A persistent imbalance in HO_x and NO_x photochemistry of the upper troposphere driven by deep tropical convection, *Geophys. Res. Lett.*, **24**, 3189-3192.
- Skamarock, W. C., et al., 2000: Numerical simulations of the 10 July STERAO/Deep Convection Experiment convective system: Dynamics and transport, *J. Geophys. Res.*, **106**, 19,973-19,990.
- Skamarock, W.C., et al., 2001: Prototypes for the WRF (Weather Research and Forecasting) Model. Preprints, *Ninth Conference on Mesoscale Processes*, Amer. Meteor. Soc., Fort Lauderdale, Florida, J11-J15.
- Wicker, L. J., and W. C. Skamarock, 2002: Time Splitting Methods for Elastic Models Using Forward Time Schemes. *Mon. Wea. Rev.*, **130**, 2088-2097.